Transactions of the Korean Nuclear Society Spring Meeting
Jeju, Korea, May 7-8, 2026

Numerical Prediction of Radial Temperature Distribution in Volumetrically Heated Turbulent Flow for MSR Flow Analysis

Moon Hyeok Kang, Jeong Ik Lee*
Dept. Nuclear & Quantum Eng., KAIST, 291 Daehak-ro, Yuseong-Gu, Daejeon 34141, Republic of Korea
*Corresponding author: jeongiklee@kaist.ac.kr

***Keywords :** Molten salt reactor, Volumetrically heated flow, Computational fluid dynamics

1. Introduction

Volumetrically heated internal flows are of practical interest in advanced nuclear energy systems, including molten salt reactors (MSRs), in which heat is generated directly within the circulating working fluid. Unlike conventional heated-wall pipe flows, the dominant thermal forcing in these systems is distributed throughout the fluid volume. As a result, the temperature field is determined by a balance among volumetric heat generation, streamwise convection associated with the non-uniform velocity profile, and radial heat transport enhanced by turbulence.

Although CFD can predict the resulting temperature distribution in detail, it is often desirable to interpret and reproduce CFD results using a reduced-order framework that is simpler, faster, and more transparent. A one-dimensional radial model provides such a framework, but it must incorporate the key effects that are implicitly captured in CFD, including turbulent thermal energy transport (through an effective conductivity) and the influence of the streamwise (i.e., streamwise) convection term that varies in perpendicular direction (i.e., radial) to the flow via the velocity profile.

In this study, a simplified one-dimensional approach for volumetrically heated pipe flow is formulated and solved numerically to obtain the radial temperature distribution under adiabatic wall conditions. The one-dimensional model is constructed by reducing the mean energy equation to a radial diffusion problem with a source term originating from volumetric heating and with turbulence represented via a closure for the effective thermal conductivity. The numerical solution of the one-dimensional model is then directly compared with RANS-based CFD results for the same geometry and operating conditions. Through this comparison, the capability and limitations of the simplified approach are assessed, and the dominant terms required to reproduce the CFD-predicted temperature profile are identified.

2. Methodology

The fluid domain was defined based on the experimental setup of Michiyoshi et al. [1]. The configuration is a vertical circular pipe with a 1 m heated section and a radius of 0.0205 m. To induce fully developed flow in the heated section, an unheated section longer than 10D is included upstream starting from the inlet. The detailed boundary conditions are shown in Fig. 1. The inlet condition is specified by prescribing the mass flow rate as Eq. (1).

$$U_{bulk} = \frac{Re\mu}{\rho D} \qquad \dot{m} = \rho U_{bulk}\frac{\pi D^2}{4} \tag{1}$$

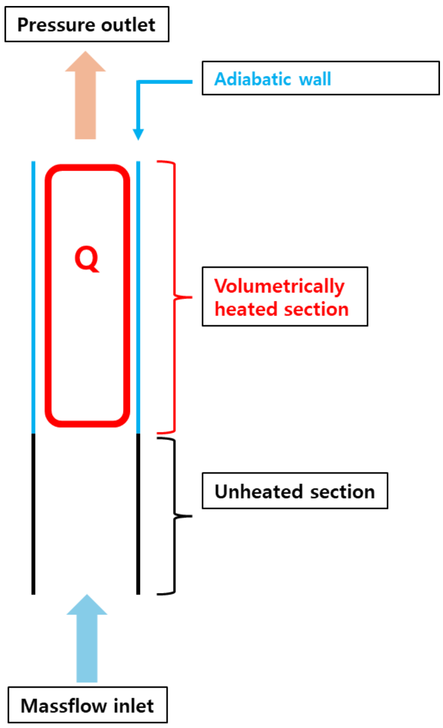

Figure 1. Fluid domain based on experiment of Michiyoshi et al.

A simulation is performed for an inlet flow at Re = 5000, and the fluid properties are set to those of seawater (Table 1), which is being consistent with the experiment conducted by Michiyoshi et al. [1].

Table 1. Thermophysical properties of the fluid

Fluid property	Value
Pr	4.41
T_{inlet} (°C)	40
ρ(kg/m^3)	1020
μ(10^{-3} Pa · s)	0.69
k(W/m · K)	0.63
β(K^{-1})	4.0×10^{-4}
c_p(J/kg · K)	4020

The governing equations for conservation of mass, momentum, and energy are given as follows. The steady, incompressible Reynolds-averaged Navier–Stokes (RANS) equations are employed as Eq. (2-5). Buoyancy is modeled using the Boussinesq approximation.

$$\nabla \cdot \boldsymbol{u} = 0 \tag{2}$$

$$\rho(\nabla \boldsymbol{u})\boldsymbol{u} = -\nabla \cdot \boldsymbol{T} + \rho \boldsymbol{g} \tag{3}$$

$$\rho c_p \boldsymbol{u} \cdot \nabla T = \nabla \cdot k \nabla T - \nabla \cdot \rho c_p \overline{T' \boldsymbol{u}'} + q''' \tag{4}$$

$$\boldsymbol{T} = -P\boldsymbol{I} + \mu[\nabla \boldsymbol{u} + (\nabla \boldsymbol{u})^T] - \rho \overline{\boldsymbol{u}' \boldsymbol{u}'} \tag{5}$$

Since the Boussinesq approximation is applied, the buoyancy term ρ$\boldsymbol{g}$ is evaluated as $\rho_{ref}\left[1 - \beta\left(\bar{T} - T_{ref}\right)\right]\boldsymbol{g}$. Here, $T_{ref} = T_{inlet}$ and $\rho_{ref} = \rho$. In addition, a uniform volumetric heat generation rate of q'''= 0.41 MW/m^3 is imposed over the heated section.

The CFD simulations were performed using ANSYS CFX 2025 R1. Turbulence is modeled with the k–ω SST model, and the turbulent Prandtl number is set to constant value. The mesh is constructed as shown in Fig. 2. Using the Sweep method provided in ANSYS Meshing, the cross-sectional mesh is extruded in the streamwise direction, resulting in identical cross-sections along the pipe length.

Three mesh levels—C (Coarse), M (Medium), and F (Fine)—were generated, and the detailed mesh information is summarized in Table 2.

Table 2. Mesh information

Mesh	Cells (M)	Base (mm)	y(mm)	y^+
C	7.03	0.8	0.13	1.06
M	11.7	0.75	0.043	0.375
F	17.6	0.7	0.02	0.174

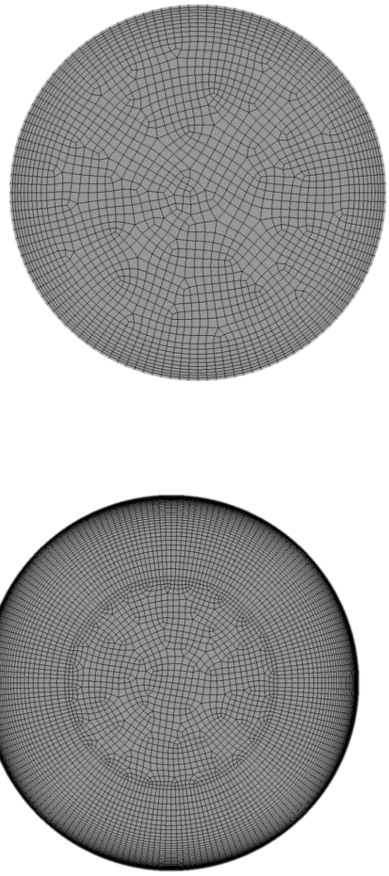

Figure 2. Meshed cross-sectional plane (top : Coarse case, bottom : Fine case)

3. Results

After performing the simulations, the radial temperature profile at the streamwise location $z/R = 22.5$ was obtained as a function of the normalized radius $(r/R = r^*)$, as shown in Fig. 3. The normalized temperature T^* is defined with respect to the volumetric heating as Eq. (6), where the subscript C denotes the centerline.

$$T^*(r^*) = \frac{T(r^*) - T_C}{q''' R^2 / 2k} \tag{6}$$

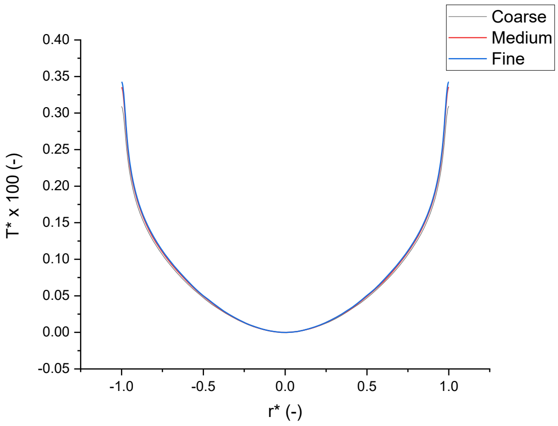

Figure 3. Radial temperature profile of normalized nondimensional temperature

According to Fig. 3, the grid-dependent asymptotic behavior is clearly observed. These CFD results can be reproduced using a simplified one-dimensional approach through a reduced numerical analysis. For a fixed z, the governing equation for temperature can be written as Eq. (7).

$$\rho c_p \boldsymbol{u} \cdot \nabla T = \nabla \cdot k \nabla T - \nabla \cdot \rho c_p \overline{T' \boldsymbol{u}'} + q''' \tag{7}$$

For a fully developed flow, the velocity vector $\boldsymbol{u} = (u, v, w)$ satisfies $u = v = 0$. The turbulent diffusion term is incorporated through an effective thermal conductivity, k_{eff}, and the equation is rearranged as Eq. (8). For pipe flow, the resulting form is expressed in the radial coordinate system.

$$\rho c_p w T_z = \nabla \cdot k_{eff} \nabla T + q''' \tag{8}$$

Although the above simplification is not strictly valid, it provides a reasonable representation of the flow-averaged behavior of T_z between the wall—where the no-slip condition applies—and the centerline. This equation can then be rewritten as Eq. (9), using the streamwise energy balance. A_C denotes the channel area.

$$\dot{m} c_p \frac{dT_{bulk}}{dz} = q''' A_C \tag{9}$$

By rearranging the equation, the equation can be expressed as Eq. (10).

$$T_z \cong \frac{q''' A_C}{\dot{m} c_p} = \frac{q'''}{w_{bulk} \rho c_p} \tag{10}$$

Hence, streamwise thermal diffusion (streamwise conduction) is neglected in the energy equation as Eq. (11).

$$T_{zz} \cong 0 \tag{11}$$

However, if the streamwise temperature gradient is approximated using the bulk temperature rise, it is underestimated near the wall because the local streamwise velocity there is much smaller. Since this near-wall deviation depends on the velocity profile, the radial temperature profile cannot be captured accurately using a single bulk-based value of the streamwise gradient.

Therefore, in the present study, an eigenvalue parameter λ is introduced. Neglecting streamwise diffusion and assuming a fully developed, axisymmetric pipe flow, the governing energy equation can be reduced to a one-dimensional problem in the radial direction (Eq. (12)).

$$(\lambda w - 1) q''' = \frac{1}{r} \frac{d}{dr} (k_{eff} r T_r) \tag{12}$$

For fully developed forced convection turbulent flow, w can be expressed as Eq. (13), which is known as Prandtl's 1/7th power law.

$$w(x, y) \propto (1 - r/R)^{1/7} \tag{13}$$

On the other hand, at $Re = 5000$ the flow is close to the transitional regime, and thus it is not appropriate to directly adopt the conventional value of $n = 7$. Therefore, n is determined using Schlichting's Prandtl's equation in Eq. (14) for smooth pipe [3].

$$n = 2\, log_{10} \left(\frac{Re}{n} \right) - 0.8 \quad n = 5.17 \tag{14}$$

Using the eigenvalue λ, the equation can be rewritten as Eq. (15).

$$(\lambda (1 - r/R)^{1/n} - 1) q''' = \frac{1}{r} \frac{d}{dr} (k_{eff} r T_r) \tag{15}$$

λ must satisfy the boundary conditions imposed on $k_{eff} r T_r$. These boundary conditions follow from the adiabatic wall condition and the fully developed flow assumption as Eq. (16).

$$r T_r (r = 0) = r T_r (r = R) = 0 \tag{16}$$

This leads to a simple one-dimensional numerical problem. The parameter λ is then determined iteratively. To close the model, an expression for k_{eff} is required, and the following closure is employed as Eq. (17-18). The turbulent Prandtl number is evaluated using the correlation of Kasagi and Myong [4], which is adopted to account for the relatively high Prandtl number in the present study.

$$k_{eff} = k\left(1 + \frac{Pr}{Pr_t}\frac{\nu_t}{\nu}\right) \quad (17)$$

$$Pr_t = 0.75 + \frac{1.63}{\ln{(1 + Pr/0.0015)}} \quad (18)$$

Here, the eddy viscosity is modeled using the Reichardt correlation (Eq. (19)) with the van Driest damping function (Eq. (20))[2].

$$\frac{\nu_t}{\nu} = \frac{\kappa y^+}{6}\left(1 + \frac{r}{R}\right)\left(1 + 2\left(\frac{r}{R}\right)^2\right)f_\nu^2 \quad (19)$$

$$f_\nu = 1 - e^{-\frac{y^+}{A^+}} \quad A^+ = 26 \quad (20)$$

In addition, to evaluate y^+, the wall shear stress and the friction Reynolds number are estimated using the Blasius correlation based on the Darcy friction factor shown in Eq. (21-23).

$$f = 0.316Re^{-1/4} = \frac{8\tau_w}{\rho U_{bulk}^2} \quad (21)$$

$$u_\tau = U_{bulk}\sqrt{f/8} \quad (22)$$

$$Re_\tau = \frac{u_\tau R}{\nu} = \frac{U_{bulk}D}{2\nu}\sqrt{f/8} = \frac{Re}{2}\sqrt{f/8} \quad (23)$$

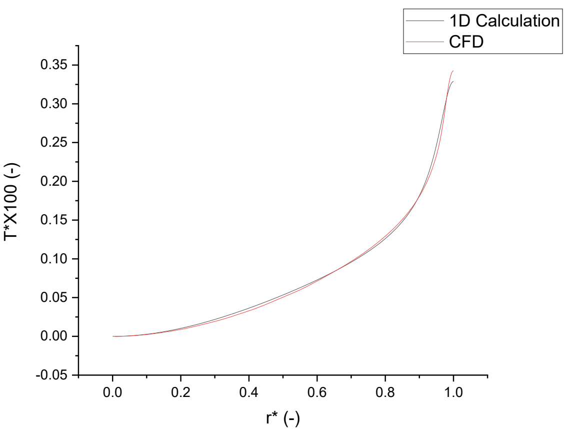

Figure 4. Radial temperature distribution obtained from CFD and one-dimensional model

As shown in Fig. 4, the radial temperature profile was obtained from the one-dimensional model, and the comparison with the CFD results shows reasonable agreement.

4. Conclusions

This study developed a simple one-dimensional numerical model for volumetrically heated pipe flow and compared its predicted radial temperature profile with CFD results under adiabatic wall conditions. The one-dimensional solution reproduced the main shape and trend of the CFD temperature distribution when turbulent heat transport and the influence of the velocity profile were represented in a consistent way.

A key step was determining the scaling parameter in the reduced model through an iterative procedure so that the governing equation and boundary conditions were satisfied. The one-dimensional model relies on turbulence-related closures, including a turbulent Prandtl number correlation and a near-wall damping function in the eddy viscosity formulation, to represent turbulent heat transport consistently with the CFD setup.

For evaluating the near-wall resolution parameter, the wall shear stress and the friction Reynolds number were estimated using the Blasius correlation based on the Darcy friction factor. Overall, the results show that a compact one-dimensional approach can provide a practical and interpretable representation of CFD-predicted temperature profiles for volumetrically heated internal flows.

In volumetrically heated turbulent flow, several modeling elements in commercial CFD remain uncertain, including the treatment of turbulent heat transport, the turbulent Prandtl number, and near-wall closure assumptions. In this context, the present study proposes a one-dimensional numerical framework as a reduced-order approach for analyzing the radial temperature distribution in volumetrically heated flow. The present comparison is limited to a preliminary qualitative comparison under the assumed modeling conditions, and direct comparison with experimental data is left for future work. Such validation will be useful for assessing the applicability of both the CFD model and the reduced-order formulation to volumetrically heated internal flows. In addition, the proposed methodology may provide a useful basis for further V&V studies, including sensitivity assessments of turbulence closures and cross-comparisons between reduced-order and high-fidelity thermal-hydraulic analyses.

ACKNOWLEDGEMENT

We would like to acknowledge the technical support from ANSYS Korea.

REFERENCES

[1] Itaru Michiyoshi, Yoshihiro Kikuchi, and Osamu Furukawa. Heat transfer in a fluid with internal heat generation flowing through a vertical tube. Journal of Nuclear Science and Technology, 5(11):590-595, 1968.

[2] W.M. Kays, M.E. Crawford, and B. Weigand. Convective Heat and Mass Transfer. McGraw-Hill series in mechanical engineering. McGraw-Hill, 2005.

[3] Schlichting, Hermann, and Klaus Gersten. *Boundary-layer theory*. springer, 2016.

[4] Myong, Hyon Kook, Nobuhide Kasagi, and Masaru Hirata. "Numerical prediction of turbulent pipe flow heat transfer for various Prandtl number fluids with the improved k-ε turbulence model." *JSME international journal. Ser. 2, Fluids engineering, heat transfer, power, combustion, thermophysical properties* 32.4 (1989): 613-622.